Proceedings of the 2010 International Conference on Condition Monitoring and Diagnosis, September 6-11, 2010, Tokyo, Japan

Propagation Mechanisms of PD Pulses for UHF and Traditional Electrical Measurements

S.M. Hoek[1*], M. Koch[1] and M. Heindl[2]
[1] OMICRON electronics GmbH Austria
[2] University of Stuttgart / Germany
*E-mail : stefan.hoek@omicron.at

Abstract — **Partial Discharge (PD) measurements are considered as a very powerful technique for testing and monitoring the condition of HV insulations. PD diagnostics is generally accepted as an early breakdown indicator, which is also reflected in numerous standards. In the present contribution, the authors describe the fundamentally different propagation mechanisms of electrical impulses in the conventional, IEC and the high, UHF frequency range. The low frequency components of the PD signals propagate mainly via the conductor whereas the high frequency components (UHF signals) are radiated as electromagnetic waves. The sensitivity and spectrum of the measurement depends strongly on the geometric position of the PD, damping and resonances of the propagation path and the frequency response of the receiver. Field simulation has been used as an appropriate tool for calculating PD signal propagation in HV apparatus.**

Index Terms – Partial Discharges (PD), Ultra High Frequency (UHF), IEC 60270, propagation mechanisms, wave and conductor guided dispersion, simulation and theory.

I. INTRODUCTION

Partial Discharge (PD) measurement is a worldwide accepted method for quality control of high voltage (HV) insulation systems [1], [2]. Partial discharges are local electrical discharges that partially break down the HV insulation [3] and generate electric impulses as well as electromagnetic waves in a broad frequency spectrum due to their short rise time and duration [4]. Measurement and detection of PD is performed with different methods involving different propagation paths, propagation mechanisms and sensor principles which result in divergent transfer behavior. The measurable signal spectrum (magnitude vs. frequency) depends directly on source geometry and location, structure of the test setup and the used sensor and measurement technology. Figure 1 illustrates the propagation of PD signals from source to receiver. The originally very wide frequency spectrum of the Dirac-like discharge spark is modified by the electric characteristics of its close surroundings, the propagation path with its damping and resonances and finally by the frequency response of the measurement system. Hence a PD measurement takes advantage of only a fraction of the original frequency spectrum.

A common setup according to IEC 60270 uses band pass filters in the range of some 100 kHz, aiming to measure in a frequency range less subject to external disturbances which are typically radiating in a broad frequency spectrum. For higher center frequencies of some 100 MHz, a fundamentally different nature of the disturbances can be expected; having often more narrowband character. However, PD pulses with their broadband spectral energy will radiate in the lower frequency range as well as in this UHF range [5]. By choosing a suitable measurement frequency range or by combining of both, the conventional and the UHF technique, external disturbances can be handled much better. This different behavior of disturbances and PD pulses and the different sensor principle lead to some advantages for the UHF-method e.g. during on-site measurements[6].

However there are general uncertainties related to the comparability of the UHF measurements to conventional IEC conformant tests [7]. For example, during Cigré Session 2008 the Special Reporter of SC D1 asked the question: "How can the relation between the conventional PD measurement and the UHF measurement determined and generalized?" [8].

In the present contribution, the authors detail the fundamentally different propagation mechanisms of electric impulses based on Maxwell's law of total current. Simulation results of PD signal propagation in GIS illustrate graphically the complex and very geometry sensitive transfer function of UHF signals. The authors conclude that a general correlation between conventional PD measurements and these in the UHF range does not exist.

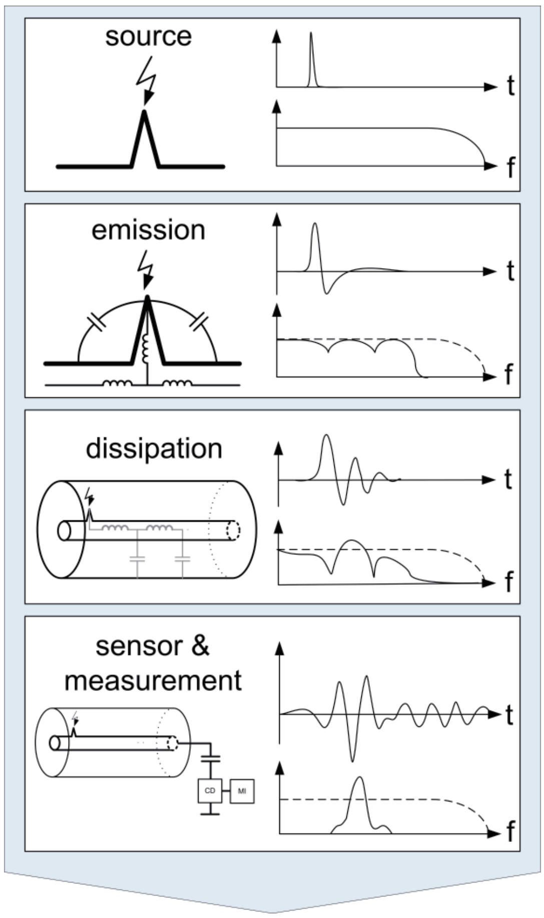

Figure 1: PD signal propagation and variation in frequency spectrum from source to test system

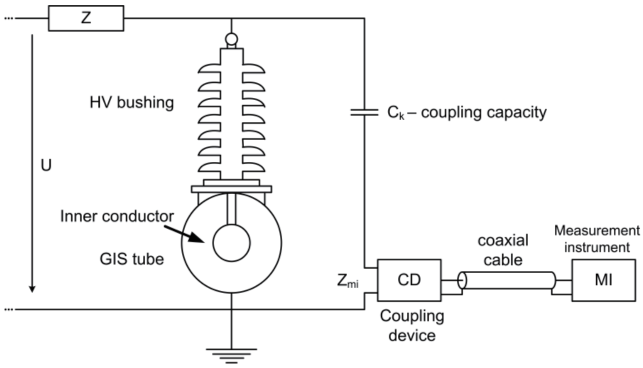

Figure 2: IEC 602070 compliant PD measurement setup.

According to the IEC 60270 standard (conventional method), the PD signals are measured with a coupling capacitor, Figure 2. With the UHF method, the PD signals are detected in the UHF frequency range with disk couplers or other antennas, Figure 3.

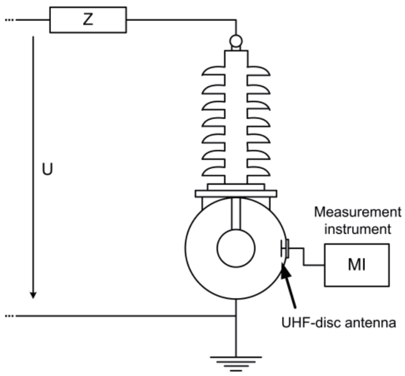

Figure 3: UHF PD measurement setup

II. Theorie of Impulse Propagation

A. Maxwell's Law of Total Currents

For describing the principles of electro-magnetic impulse propagation, one may start with the famous equations of Maxwell. An electrical field *E(t)* generates a current density *J(t)* as a sum of conduction and displacement currents, where σ_0 is the volume conductivity of that material. From (1) it can be concluded that

- Electrical conduction consists of two phenomena, where one is related to a conductor and the other to an insulating medium existing between the conductors.
- The second phenomenon, displacement current, is particularly present for fast variations of *d/dt*, that is for high frequencies and leads to electromagnetic wave propagation.

$$\nabla \times H(t) = J(t) = \sigma_0 E(t) + \frac{dD(t)}{dt} \quad (1)$$

B. Signal Propagation for Low Frequencies

The propagation of PD signals with small frequencies in conductors usually takes place by conduction currents. In a conductor, the surrounding magnetic field is closed. The electric field has its origin on the conductor surface and spreads radially. Neither H-field nor E-field have components in the direction of propagation. This corresponds to the definition of propagation of the TEM mode, able to propagate from DC to very high frequencies

C. Electro-Magnetic Wave Propagation

For higher frequencies, it comes to wave propagation as soon as the wavelength of the signal is in the order to the conductors length. This means that for high frequencies the conductive structure works increasingly as an antenna, which cut-off frequency depends on the length. Correspondingly, the structure of the PD source influences the PD signal.

D. Resonances and Wave Mode

The transfer function (and so the sensitivity vs. frequency of a measurement) is significantly influenced by resonances. These are caused by the capacitance and inductance of the propagation path, and can be installed discreetly or originate from geometric conditions.

Three different types of wave modes propagate in cavities with conductive boundaries like transformer tank [9], GIS, etc: The TM_{mn}-mode ($H_X = 0$), the TE_{mn}-mode ($E_X = 0$) and the TEM-mode ($H_X = 0$, $E_X = 0$), where m and n mark the different types of wave modes. Every wave mode, except the TEM-mode, has its own critical frequency (f_c). TE or TM modes propagate at frequencies above their own critical frequency / cut-off-frequency (f_c). TEM-modes have no critical frequency and will propagate starting from 0 Hz. However their energy decays with increasing frequency. The critical frequencies depend directly on structure geometry (e.g. GIS diameter, side lengths or transformer housing together). With an increasing cross section of the GIS, the critical frequency is decreasing. In Figure 4, the critical frequencies of the first wave modes are shown for three different geometries, respective different types of GIS [10].

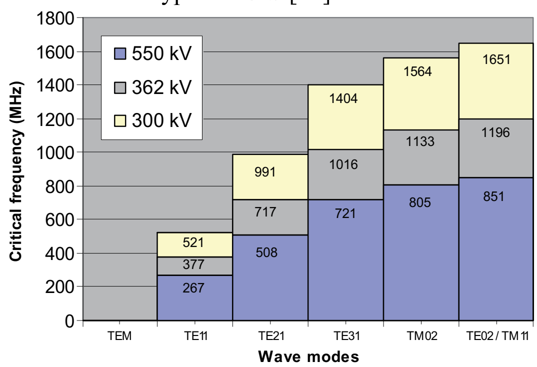

Figure 4: Critical frequencies (f_c) within a GIS for 300 kV, 362 kV and 550 kV [11].

The complexity is further increased by considering (2) the frequency dependence of the group velocity (v_g) of the TE- / TM-wave modes especially around their cut-off-frequency [11] (c_0 is the speed of light).

$$v_g(f) = c_0 \cdot \sqrt{1 - \frac{f_c}{f}} \quad (2)$$

III. Simulation of PD Signal Propagation in GIS

A. Simulation Model

In order to investigate characteristics of the two common PD measurement principles, a simulation model of a gas insulated switchgear (GIS) was created using CST Microwave Studio (MWS) software package. MWS uses finite integration technique (FIT) to solve electromagnetic field problems in time domain [12]. It is suitable to simulate electromagnetic wave propagation mechanisms through air and wire within electrically large structures like GIS. Figure 5 shows an overview of the simulation arrangement. The model consists of an evacuated tube of 7.4 m length with diameter of 55 cm and a centered inner conductor tube with 16 cm diameter. The inner conductor is held in position by 3 epoxy resin spacers (assumed $\varepsilon_r = 4.0$). Both ends of the GIS are terminated with so-called waveguide ports which are adapted to the characteristic wave impedance of the arrangement. This technique provides absorption of wave energy and inhibits total reflection at both end of the structure; otherwise reflections would keep electromagnetic waves propagating through the arrangement over and over again without decreasing of the overall field energy, which is an unrealistic boundary condition.

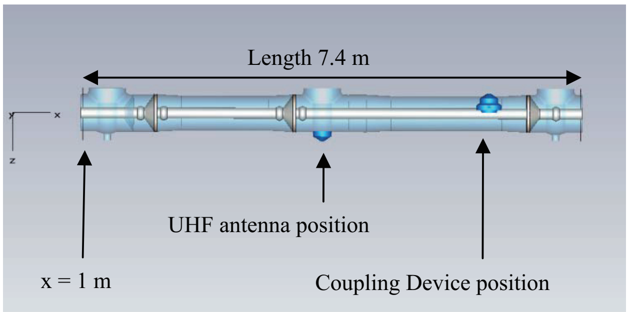

Figure 5: GIS model overview in CST MWS

The injection of PD pulses into the inner conductor of the GIS, i.e. simulation of a PD source, was carried out by an additional insulated spherical conductor between the inner and outer conductor tubes, see Figure 6. A pulse voltage source connects the inner conductor of the GIS with the sphere. This composition fulfills two purposes:

- Radiation of electromagnetic waves as they are caused by real PD sources
- Injection of a “PD current” into the inner conductor

As described above, decoupling of the PD signals is done in two different ways. Firstly, a coupling capacity with a coupling impedance in series (referred to as coupling device, CD) provides monitoring of line coupled signals of the inner conductor. Both for the conventional CD and the UHF antenna, PD signals can be recorded by monitoring voltage and current through lumped elements.

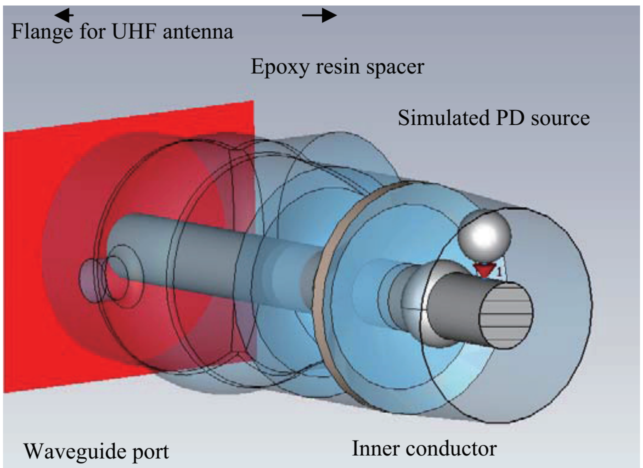

Figure 6: PD source model inside GIS represented in YZ-plane section

B. Simulation Results

Two different experiments (calibration experiment and IEC & UHF combined measurement experiment) were simulated with the model. First, a calibration signal was injected at four different positions using a lumped element capacitor (100 pF) connected to the inner conductor with a voltage source in series connected to the grounded outer tube. The applied unipolar Gaussian voltage pulse of 1 V magnitude causes a bipolar current pulse propagating through the inner conductor and is regarded to stand for an apparent charge level of 100 pC. Even for large structures like GIS, its amplitude is almost independent of the position of injection.

The second experiment simulates a PD event using the spherical structure described above as PD source

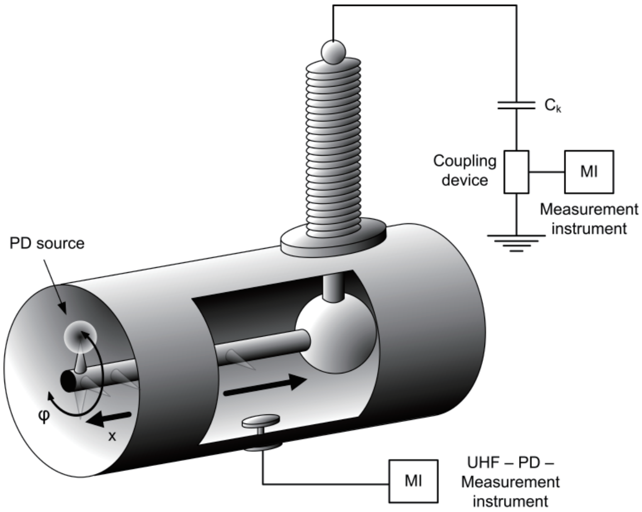

Figure 7: Variation of PD source position inside GIS and simultaneous PD measurement (UHF and conventional method)

The position of the PD source is defined by its x-position and angle within the yz-plane. First the x-position of the PD source was varied while the angle φ was left constant; second the angle was varied while the x-position was kept constant (see Figure 7).

Figure 8 shows the measurable UHF antenna peak voltage and apparent charge level when the x-position was varied

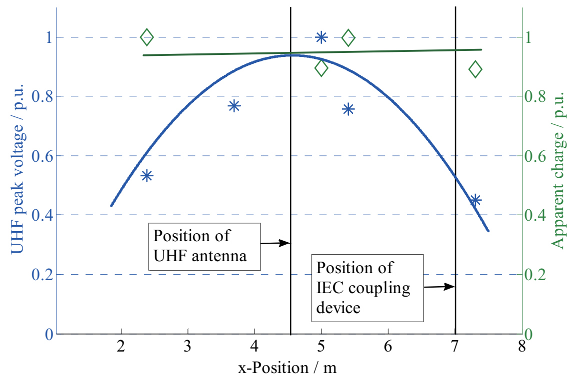

Figure 8: UHF peak voltage and apparent charge level vs. x-position of simulated PD source

Signal damping clearly increases with distance between UHF antenna (fixed position) and PD source. The apparent charge level shows only minor sensitivity to the position of the PD, due to resistive and inductive damping. Figure 9 shows apparent charge level and peak voltage picked up by the UHF antenna when the x-position of the PD source was kept constant and its angle φ was varied in steps of 90°. Again, the apparent charge level remains almost constant while the UHF peak voltage varies by almost 25 %.

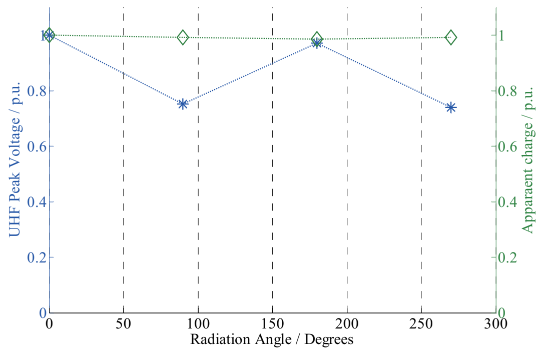

Figure 9: UHF peak voltage and apparent charge level vs. radiation angle φ of PD source

This can be explained by the complex wave propagation mechanisms for signals in the UHF range.

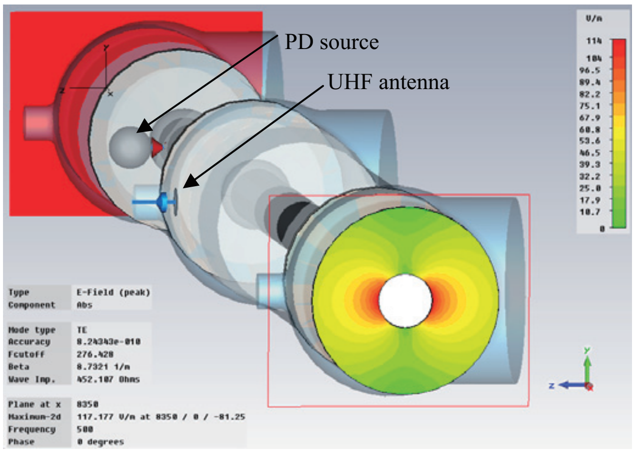

Figure 10: Electrical field distribution of TE_{11} wave mode inside GIS

This effect is explainable by wave modes inside of the GIS. The field components in the direction of propagation of the TE / TM - modes results in a angel dependence of the field distribution in the yz-plane as it is shown in Figure 10.

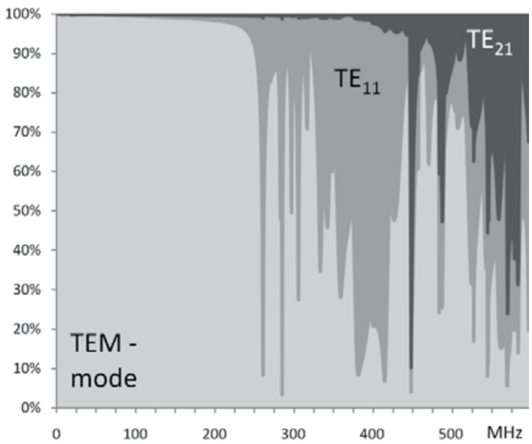

Figure 11: Share of the TEM-wave modes and higher modes (TE_{11} and TE_{21}) at the total transfer function versus the frequency

The analysis of the energy distribution of the single modes (at waveguide port) shows a shift to higher modes for higher frequencies. The dominant importance of the TEM or the propagation through conductors is reduced to the higher modes e.g. in GIS.

Figure 11 clearly shows that there is an exclusive TEM-mode transfer up to the cut-off frequency of the first higher mode (TE_{11}). For higher frequencies the importance of higher modes depends on the geometry. Generally, if the impulse is broadband enough to stimulate the electric magnetic wave, cavity resonances or other resonances must this be considered.

IV. Conclusions

- The low frequency components of the PD signals propagate mainly via the conductor. In large setups, the damping of the signal is not always negligible during calibration and measurement.
- The high frequency components (UHF signals) propagate through electromagnetic waves.
- The sensitivity of the measurement and spectrum of the measurement depends strongly on the geometric position of the PD, damping and resonances of the propagation path and the frequency response of the receiver.
- Field simulation has been used as an appropriate tool for calculating PD signal propagation in HV apparatus.

V. References

[1] D. König and Y.N. Rao: "Partial Discharges in Electrical Power Apparatus", VDE 1993

[2] J.C. Montanari: "Insulation diagnosis of high voltage apparatus by partial discharge investigation", Liu-Yeda Memorial Lecture, in Proc. IEEE ICPADM, Bali, Indonesia, 2006

[3] IEC 60270, "High-voltage test techniques – Partial discharge measurement", Version 2000, 3rd Edition

[4] M.D. Judd, S. Meijer and S. Tenbohlen, "Sensitivity check for RF PD detection for power transformers," IEEE Conference on Condition Monitoring and Diagnosis (CMD), Peking, China, April 21-24, 2008, paper No. K1-03

[5] Judd, M.D.; Farish, O.; Hampton, B. F. (1996) "The Excitation of UHF Signals by Partial Discharges in GIS", IEEE Transactions on Dielectrics and Electrical Insulation, Vol. 3 No. 2, April 1996,

[6] Markalous, S.M., Tenbohlen,S., Feser,K.: "Detection and Location of Partial Discharges in Power Transformers using acoustic and electromagnetic signals". IEEE Tr. on Dielectrics and Electrical Insulation, Vol. 15, No. 6, pp. 1576-1583

[7] S.M. Hoek, S. Coenen, M. Bornowski, S. Tenbohlen: "Fundamental Differences of the PD Measurement according to IEC 60270 and in UHF range", 2008 International Conference on Condition Monitoring and Diagnosis, Beijing, China, April 21-24, 2008

[8] J. Densley et al. "Special Report for Group D1", Cigré Main Session 2008, online available at www.cigre.org

[9] S. Tenbohlen, S.M. Hoek, D. Denissov, S.M. Markalous, "Partial Discharge Measurement in the Ultra High Frequency (UHF) Range," IEEE Tr. on Dielectrics and Electrical Insulation, Vol. 15, No. 6/2008, pp. 1544-1552

[10] R. Kurrer, K. Feser, "The Application of Ultra-High-Frequency Partial Discharge Measurements to Gas-Insulated Substations", IEEE Transactions on Power Delivery, Vol. 13, No. 3, July 1998

[11] S.M. Hoek, U. Riechert, T. Strehl, K. Feser, and S. Tenbohlen, " New Procedures for Partial Discharge Localization in Gas-Insulated Switchgears in Frequency and Time Domain ", ISH Ljubljana / Slovenia, August 2007

[12] I. Munteanu, M. Timm, T. Weiland, "It's About Time," Microwave Magazine, IEEE, vol. 11, issue 2, pp. 60–69, March 2010.